Materials Science-Poland, Vol. 22, No. 4, 2004

Spectral and microscopic examinations of metalloporphyrin-labelled polymers on different substrates

ANDRZEJ BOGUTA[1*], DANUTA WRÓBEL[1], YURI S. AVLASEVICH[2], RONALD RIES[3], ASTA RICHTER[3]

[1]Institute of Physics, Poznan University of Technology, Nieszawska 13A, 60965 Poznań, Poland

[2]Institute of Molecular and Atomic Physics, National Academy of Sciences of Belarus, 70 F. Skaryna Ave., 220072 Minsk, Belarus

[3]Laboratory of Surface Science, University of Applied Sciences Wildau, Bahnhofstr. 1, 15745 Wildau, Germany

The topography of quartz and semiconducting (In_2O_3 and SnO_2) surfaces coated with a dye–polymer layer was investigated with optical microscopy and scanning force microscopy. The following macromolecular systems were used in the experiments: copper or zinc porphyrins covalently linked to polyethylene glycol (PEG) or polyisopropylacrylamide (PNIPAM) polymers. It was shown that images of the surface topography are closely connected with the relation between the magnitude of substrate grains and geometrical size of the dye–polymers. The dye–polymer layer, based on the PNIPAM polymer, shows a ring-like structure, whereas the sample based on the PEG polymer is characterized by a longitudinal dendritic topography. When the dye–polymer layer was deposited on the surface, absorption spectroscopy in polarized light was used to determine dye orientation with respect to the substrate surface. The tilt angle between the dye layer and substrate was estimated. A correlation between the substrate surface topography and the molecular arrangement of dyes is also discussed.

Key words: *light microscopy; electronic spectroscopy; scanning force microscopy; "smart" polymers; surface image*

1. Introduction

Organic dye-labelled polymers are perfect molecular systems which find a wide range of applications in science, technology and medicine [1, 2].The family of por-

[*]Corresponding author, e-mail: bogan@phys.put.poznan.pl.

phyrins and phthalocyanines constitutes a group of dyes that are very good agents as photoconverters in solar devices and as photosensitisers in photodynamic therapy and cancerous tissue diagnostics. They can also be used as molecular systems modelling biological objects (e.g. in photosynthesis) [3, 4]. On the other hand, "smart" polymers are also the subject of extensive investigations due to their particular physical properties (e.g. a wide range of electrical conductivity), and they can also serve as models of biomimetic systems (proteins, lipid–protein complexes) [5, 6]. Since porphyrin dyes and polymers are interesting objects for investigations, and they can be quite easily chemically modified to provide a wide variety in their molecular structure (and thus modifications in their physical, photophysical, and photochemical properties), a system of porphyrin macrocycles bound with polymer chains could potentially be very useful in photovoltaics and optoelectronics. Therefore, copper and zinc porphyrins covalently linked to a polymer chain are the subject of our present investigations.

In a recent study, it has been stated that only the dye layer that is in close contact with the semiconducting electrode is involved in photoelectric processes [7]. Some photophysical processes, such as charge separation upon light illumination, electron injection, etc., can occur at the dye layer–semiconductor interface, and it has been shown that the dye effectiveness in photoconversion also depends on the kind of substrate and its roughness [8, 9].

Therefore, in this paper, we focus our attention on the topography of porphyrin -labelled polymer layers on solid substrates. Some photophysical properties of dye –polymer thin layers were also investigated. As far as we know, the topography of such polymer–dye species has never been investigated by optical microscopy or scanning force microscopy (SFM). These methods are especially useful techniques for studying the topography of solid substrates, the sizes of their grains, the formation of islands, and surface roughness.

The results presented in this paper could be essential in the study of the electronic processes occurring in dye–sensitised solar cells and in optoelectronics.

2. Materials and methods

The molecular systems under investigation are copper (CuTPP) and zinc (ZnTPP) complexes of 5-(4-pyridyl)-10,15,20-tri(4-methoxy-phenyl)porphyrin, covalently bound to polymers: CuTPP connected with poly(N-isopropylacrylamide (PNIPAM copolymer) (samples **1** and **2**), and ZnTPP linked to polyethylene glycol 6600 (PEG polymer) (sample **3**). The synthetic procedure for the samples **1** and **2** was similar to that described in Refs. [10, 11], and the molecular structures of the investigated macromolecules are shown in Fig. 1. Systems **1** and **2** differ in the distance between the porphyrin dyes and length of the polymer chains, and thus also in the average distances between dyes linked to the polymer chains. The *x*/*y* ratios in polymers **1** and **2** are 330 and 2678, respectively (Fig. 1). Sample **3** was synthesised as described below.

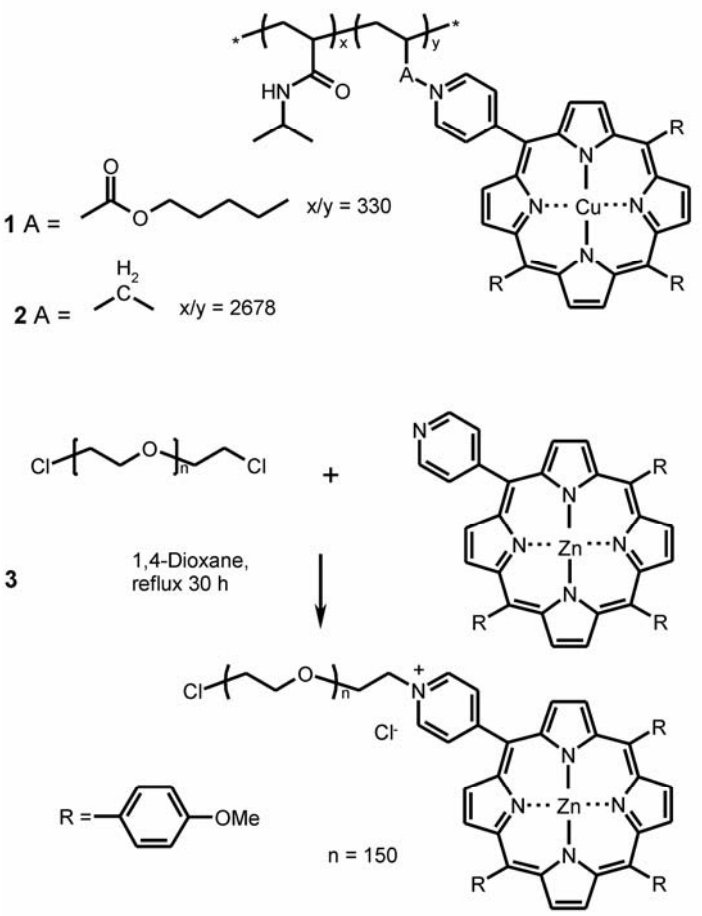

Fig. 1. Molecular structures of the investigated samples

Commercial PEG-6600 was purchased from Serva Co. 5-(4-Pyridyl)-10,15,20 -tri(4-methoxyphenyl)porphyrin and synthesized as described previously [11]. It exhibits satisfactory ^{1}H NMR data [11]. Thionyl chloride was purchased from Aldrich Chemical Co. For the synthesis, reagent-grade solvents were used without further purification, except for tetrahydrofuran (THF), 1,4-dioxane, and pyridine, which were distilled from calcium hydride.

2.1. Preparation of Cl-Modified PEG-6600

0.21 ml (3 mmol) of thionyl chloride was added under stirring at room temperature to 6.6 g (1 mmol) of PEG-4000 and 0.22 ml (3 mmol) of pyridine dissolved in 30 ml of THF. After 24 h, the solution was refluxed for 1 h and treated with active carbon (1 g). Carbon was filtered off and washed with hot dioxane (2×10 ml). The combined

filtrates were evaporated to 10 ml and cooled to room temperature. Hexane (100 ml) was added to the solution and well mixed. The obtained precipitate was filtered off, washed with hexane (2×20 ml), and dried *in vacuo* at room temperature. Yield 6.16 g (93.3%). Anal. $(C_2H_4O)_{148.6}C_2H_4Cl_2$ $(44)_{148.6}$+99: Calcd. C 54.10, H 9.01, O 35.82; Found C 54.11, H 8.74, O 35.67. IR (KBr, cm^{-1}) 735 (ν C–Cl).

2.2. Preparation of porphyrin-labelled PEG-6600

Cl2-PEG-6600 (66 mg, 10-5 mol) and Zn-5-(4-pyridyl)-10,15,20-tri(4-methoxyphenyl)porphyrin (7.6 mg, 10-5 mol) were dissolved in 1,4-dioxane (8 ml). The reaction flask was shielded from ambient light and the resulting solution was magnetically stirred under reflux for 30 h. It was cooled to room temperature and then hexane (50 ml) was added. The purple suspension was filtered, washed with hexane (2×10 ml) and dried in vacuo at room temperature. Yield 49.2 mg (66,6%). It was dissolved in a minimal volume of dioxane and then precipitated by hexane to purify the labelled PEG from the porphyrin traces.

Elementary microanalysis was performed using a Vario ELIII device. The porphyrin units content in the samples (Fig. 1) was calculated from the absorption of polymers solution in dioxane, with the use of Cu-TPP and Zn-TPP extinction coefficients [12] (absorption spectra were taken with a Varian UV-Vis-NIR Cary 500 Scan spectrophotometer, and IR spectra were recorded with a Specord 75 IR spectrophotometer). The relationships between dye and polymer absorption band intensities depend on the average amount of dye molecules per unit polymer chain (x/y).

In our experiments, the following substrates were used: a quartz plate and two semiconductors (In_2O_3 and SnO_2) deposited on a quartz plate. The semiconducting (In_2O_3 or SnO_2) substrates were deposited by evaporation onto a quartz plate. Since the investigated dye-containing polymers have a high solubility (e.g. in water), it is impossible to prepare Langmuir and Langmuir–Blodgett films of such compounds. Therefore, the modified dynamic deposition method was applied for preparing thin organic films on the quartz or semiconducting substrates [13–15]. In our experiments, chloroform was used for the dynamic deposition on solid substrates. In sample preparation, 100 μl of the dye solution in chloroform (c = 1 mM) was deposited on the cleaned substrate. The solution was spread over the solid substrate, which was set at 25 degrees with respect to the ground. The solid film was obtained as a result of chloroform evaporation during the lamellar flow of the solution. The thickness of the deposited dye layer was about 20 nm (estimated on the basis of the SFM studies).

Polarized absorption spectra for the dye layer were measured in the range of 400–900 nm with a Specord M40 UV-Vis spectrophotometer. The reference sample was a proper substrate without dyes. The dye concentration was 1 mM for sample preparation. The accuracy of the absolute absorbance intensity was 0.001. Two absorption components were measured: $A_{\parallel}$ and $A_{\perp}$ ($A_{\parallel}$ and $A_{\perp}$ are the absorbance components measured for the light electric vector parallel and perpendicular to the deposi-

tion direction of the layer, respectively). $A_{\parallel}$ and $A_{\perp}$ were measured in two geometrical arrangements:

- with the light beam perpendicular to the sample surface ($\beta = 0°$),
- with the light beam inciding at $\beta = 10°$.

Such an experimental approach allows the molecular arrangement to be determined with respect to the substrate surface, according to the method of Yoneyama et al. [16], using the following equation

$$\left\langle \cos^2 \theta \right\rangle = \frac{D_0 - \left(1 + D_0 \sin^2 \beta\right) D_\beta}{\left(1 - 2\sin^2 \beta\right) D_\beta - \left(1 + D_\beta \sin^2 \beta\right) D_0} \tag{1}$$

where $i = 0°$ or β, and θ is the angle between the molecular skeleton (assuming that the absorption transient moment lies in the dye molecular scaffold) and substrate surface; $D = A_{\parallel}/A_{\perp}$.

The linear dichroism was defined as [17]

$$LD = \frac{A_{\parallel} - A_{\perp}}{A_{\parallel} + 2A_{\perp}} \tag{2}$$

The fluorescence spectra of the investigated polymers were measured with a steady-state spectrofluorometer Hitachi F4500. The experimental arrangement of such measurements for the dye layers on the solid plates was as described in [18].

The optical microscopy images were obtained using a micro-optical 3D measuring device (GFM, Teltow, Germany). SFM measurements were performed with a Nanoscope IV in air at room temperature. The images were obtained using a standard Si_3N_4 microtip with a force constant of 0.38 $N \cdot m^{-1}$. An applied force of about 10 nN was estimated from the signal of the feedback set point. This is only an approximate measure, since the capillary condensation contributions between the tip and the surface layer are unknown. All images were obtained at the scanning rate of 2.54 Hz. None of the features in the micrographs were changed when the scan rate was varied around this value. The best results were obtained in the SFM contact mode. No damage in the molecular coating was observed after several scans.

Investigations with SFM give two types of micrographs: a deflection and height picture. Deflection images were obtained from the data that came from the differential signal of the SFM photodiode pair. The *z* (height) piezo voltage set by the feedback calculation in the digital signal processor was used to produce the height image. This image was thus caused by a signal of the difference between the loop error and point set control. The image, therefore, showed the edges clearly. The height picture was used to analyse the roughness of the samples. However, topographical features can be seen best from the deflection pictures, and these are given in this paper [19, 20].

The roughness parameter R_a was determined as an average value in a sample area of $1 \times 1\ \mu m^2$. R_a is the arithmetical mean line deviation or the so-called centre line av-

erage. It is defined as the arithmetic average over all absolute values of height h_i with respect to a reference line [20, 21] and can be measured automatically within SFM.

3. Results

3.1. Electronic spectroscopy

Figure 2 shows the polarized absorption spectra ($A_{\parallel}$ and $A_{\perp}$) of dye–polymer films on a quartz plate as an example. The bands that range between 400 and 900 nm are assigned to the dye moieties, whereas polymers are responsible for absorption in the range of 200–300 nm (not shown). The absorption spectra of the dyes on solid substrates are more or less changed with respect to dye–polymers dissolved in water [1, 11, 22]. Slight shifts of the Soret bands (2 nm for samples **1** and **2**, 5 nm for the

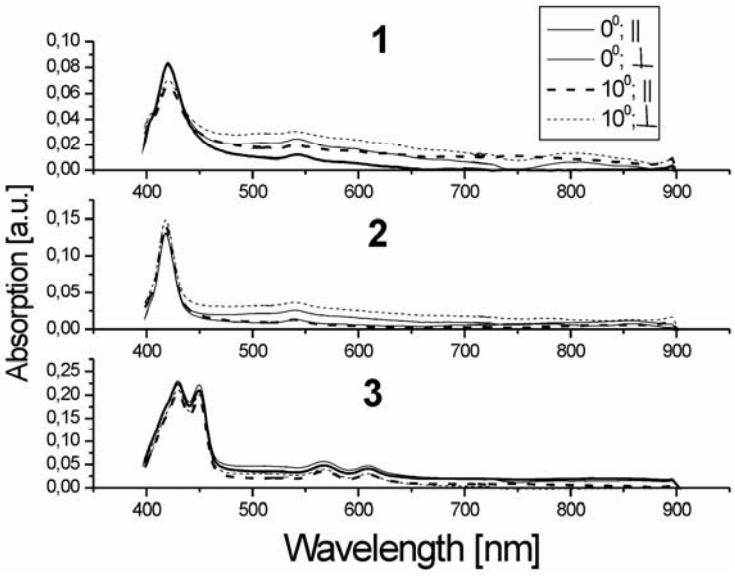

Fig. 2. Polarized absorption spectra of the dye–polymer films on quartz plates. The absorption components $A_{\parallel}$ and $A_{\perp}$ were measured with a light beam perpendicular to the sample surface (0°) and with the light beam inciding at 10°

polymer **3**) are assigned to the interaction of the dye–polymer with the solid surfaces. For the polymer **3**, the splitting of the Soret band is observed – the band intensity (the ratio of the band at 425 nm and 449 nm) changes as compared to that in aqueous solution [1, 22]. This band splitting could be assigned to a strong interaction between dye moieties, which are close to one another, as observed for strongly interacting molecules. The shapes of the spectra for the remaining substrates (In_2O_3 and SnO_2) are

essentially unchanged (not shown). The relative intensities of these bands, however, are altered when thin films are deposited on quartz, In_2O_3, or SnO_2 plates. This indicates that the interaction between the dye molecules and polymer chains is disturbed in different ways by various solid substrates. It can also be due to a different dye orientation with respect to the solid surface.

On the basis of polarized absorption measurements, the orientation of dye molecules on the solid surface can be evaluated. We begin with a description of the orientation of sample **3** on quartz, In_2O_3 and SnO_2. The first interesting feature is that the perpendicular component ($A_\perp$) is a little higher in intensity than the parallel one ($A_\parallel$). This indicates that the dye molecules are oriented rather perpendicular to the substrate surface. Such an arrangement of the porphyrin dyes is supported by the values of the linear dichroism (LD) parameters. The corresponding tilt angles and LD parameters are given in Table 1. We realize that our estimation is rather rough due to small difference between $A_\parallel$ and $A_\perp$ and due to the low absorbance of dyes in the thin films. Nevertheless, the data in Table 1 show a tendency of the dye molecules to be arranged in an out-of-plane orientation. In our previous paper, we have also investigated the orientation of porphyrin dyes in a form of the Langmuir or Langmuir –Blodgett layers [9]. A flat arrangement of the LB dye layer (without polymer) on solid In_2O_3 and SnO_2 was shown [9]. The estimated angles were from 24° to 33° in the Langmuir–Blodgett layer [9], whereas in this paper the angles lie between 56° and 68°. For a similar porphyrin, the variation in the tilt angles on the same substrates could be assigned to the large influence of the polymer skeleton **3** on the orientational behaviour of the dye molecules.

Table 1. Linear dichroism (LD)[1] values of dyes on different substrates and the angles θ between the dye molecular skeleton and substrate surface

Sample	LD			θ, deg		
	Substrate					
	Quartz	In_2O_3	SnO_2	Quartz	In_2O_3	SnO_2
1	0.030	0.050	0.020	26	9	13
2	-0.010	0.030	0.110	68	7	32
3	-0.010	-0.010	-0.010	68	56	61

[1]LD estimated at the maximal dye absorbance. $\Delta LD = \pm 0.005$, $\Delta\theta = 3°$.

On the other hand, the dye molecules are rather in-plane oriented when linked to the other polymer chains (samples **1** and **2**). The estimated tilt angles range between 70 and 320 (except for polymer **2** on the quartz plate). In comparison with our previous LD observation for porphyrin molecules in the LB film on In_2O_3 and SnO_2 substrates [9], the arrangement of the dye molecules is also disturbed by the presence of the polymers. This conclusion is supported by the data presented in our previous paper for the porphyrin molecule in the absence of polymers (**1** and **2**) [9].

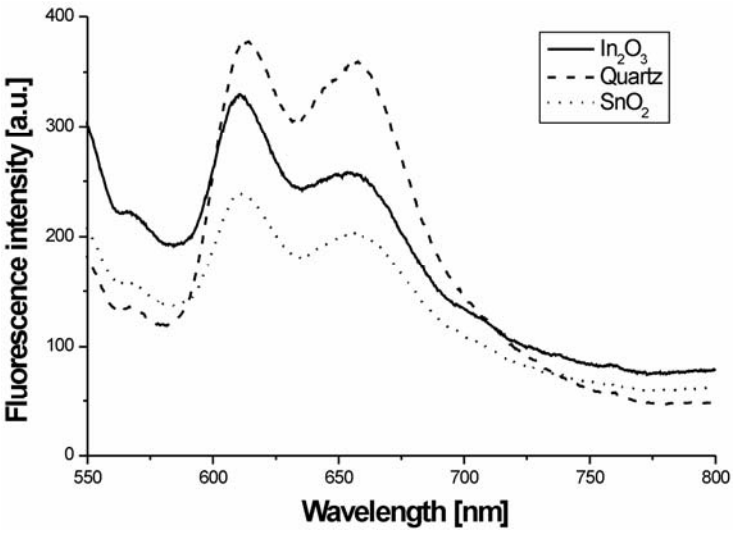

Fig. 3. The fluorescence spectra of dye–polymer **3** on various substrates

The dye–polymer species studied do not show any fluorescence in aqueous solution (or it is extremely low; data not shown). The fluorescence features are dramatically changed after depositing the dye layers on the solid substrates. Figure 3 shows examples of the dye–polymer **3** on quartz, In_2O_3 and SnO_2. Two bands, typical of porphyrin dyes, are observed. One band is located around 610 nm and the other at about 650 nm. The band locations are different from those obtained for the dyes in, e.g. DMSO [9]. Also, the bands are much broader than those observed for these dyes dissolved in organic solvents [9, 23]. This means that the interaction of the dye–polymers with the solid surface affects their fluorescence behaviour. In the previous work [24], the infrared spectroscopy showed the charge redistribution in the dye macrocycles after dye Langmuir–Blodgett layer formation. We can thus suppose that electronic interaction between π electrons in the dye skeleton and the solid is the reason for the enhanced dye fluorescence observed in this paper.

Summarizing, we conclude that the dye arrangement in thin films on the solid substrates depends crucially on the substrate material. The most important observation is that the dye orientation is altered in the presence of the polymer chains. A marked variation in dye arrangement is shown for the ZnTPP dye linked to the polymer system (**3**). We thus suggest that the molecular arrangement and electronic interactions in the dye–polymer systems could affect the final topography of the thin film.

3.2. Microscopic studies

In our experiments, we use three solid substrates: a quartz plate, and In_2O_3 or SnO_2 deposited on the quartz plates. Previously, the differences in their topographies were shown and they were characterized by a different size of grains [9]. The quartz plate

had a very smooth surface with the lowest roughness parameter (R_a = 0.1 nm), In_2O_3 on quartz was characterized by low surface granularity (R_a = 0.4 nm), and the SnO_2 layer exhibited the highest value of the roughness parameter (R_a = 2.2 nm). The same substrates were used in this paper, and their images are comparable with those presented in the previous paper [9].

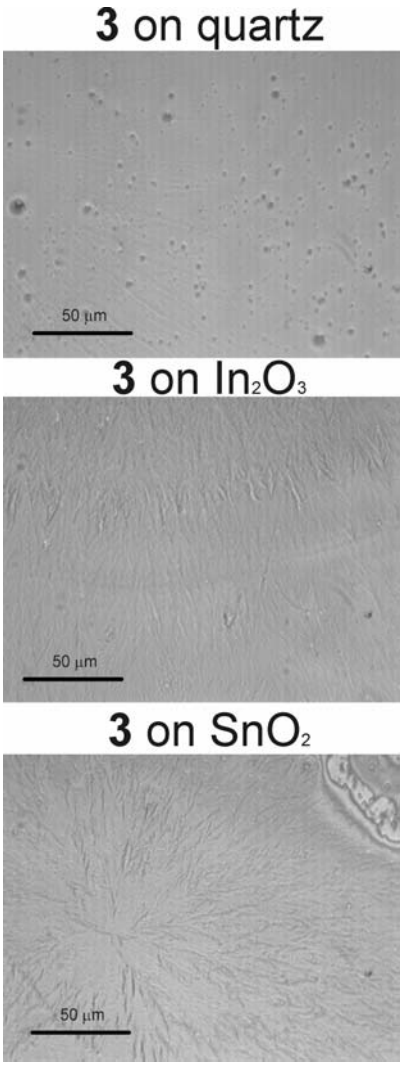

Fig. 4. Optical microscopy images of **3** on quartz, In_2O_3 and SnO_2

Deposition of sample **3** on the quartz plate and on In_2O_3 and SnO_2 (Fig. 4) leads to differences in the macroscopic images. A marked variation in the topography of the dye–polymer system **3** is observed as compared to the images of the substrates [9].

A dendritic structure of the polymer film, with crystallization centres, can be seen (on In_2O_3 and SnO_2 substrates). Its character depends on the granularity of the original surfaces. The higher the roughness parameter, the larger are the visualised dendritics and crystallization grains.

For samples **1** and **2**, rather smooth homogeneous surfaces are observed, and the differences between the surface structures of these samples on quartz and SnO_2 are due to variations in the grain sizes of these two solid substrates (data not shown).

In summary, we conclude from this part of the paper that the dye–polymer systems **1** and **2** present rather homogeneous topographies, while the dye–polymer **3** exhibits a dendritic topography and its final image depends on the granularity of the solid surface.

A deeper insight into the topography of dye–polymer systems can be obtained from SFM experiments, since SFM visualization gives much more details than optical microscopy. The SFM images of samples **1**, **2**, and **3** on SnO_2 give very similar images (not shown). For each dye–polymer on SnO_2, an image of the substrate is observed rather than the individual character of the polymer layer owing to the large granularity of SnO_2. Detailed SFM images of the film are thus impossible to obtain due to the high roughness of the SnO_2 substrate.

Much more interesting results were obtained for dye–polymer films deposited on substrates of low granularity – on quartz and In_2O_3. Figures 5–8 show the results for samples **1** and **3**, respectively, on quartz or In_2O_3. A comparison of these figures evidently shows that the final SFM images depend strongly on the dye–polymer and the granularity of the solid substrate. For sample **1**, a ring-like topography is observed (Fig. 5). The sequences of the rings are repeated along the whole sample. In the panel in Fig. 5, a cross-section analysis of this structure is presented. The size of the polymer could be estimated basing on the evaluation of the roughness parameters for the bare substrates. The height of the polymer is about 9–11 nm. The diameter was estimated to be about 450 nm.

Small changes can be observed in the SFM images when the porphyrin–polymer **1** covers the In_2O_3 surface. Figure 6 shows the SFM image of this sample on In_2O_3, with the section analysis of the image also shown. Again, a ring-like structure could be recognized, but it is not as clear as for the same dye–polymer on quartz. Cross-section analysis gives the height values 12 and 17 nm. These values could be described as follows. On the basis of our previous results concerning SFM images of the In_2O_3 substrate, the height of In_2O_3 grains was estimated to be about 5–7 nm. The first cross section value (12 nm) can thus be assigned to the thickness of polymer layer that is in contact with the In_2O_3 grain pit. The higher value (17 nm) reflects the height of the polymer layer on top of an In_2O_3 grain. This value is higher than that for the same sample on quartz, as expected. The variations in the SFM images of sample **1** on In_2O_3 and quartz and the differences in height could be caused by either a difference in grain size between the two substrates or by a different dye orientation with respect to the substrates.

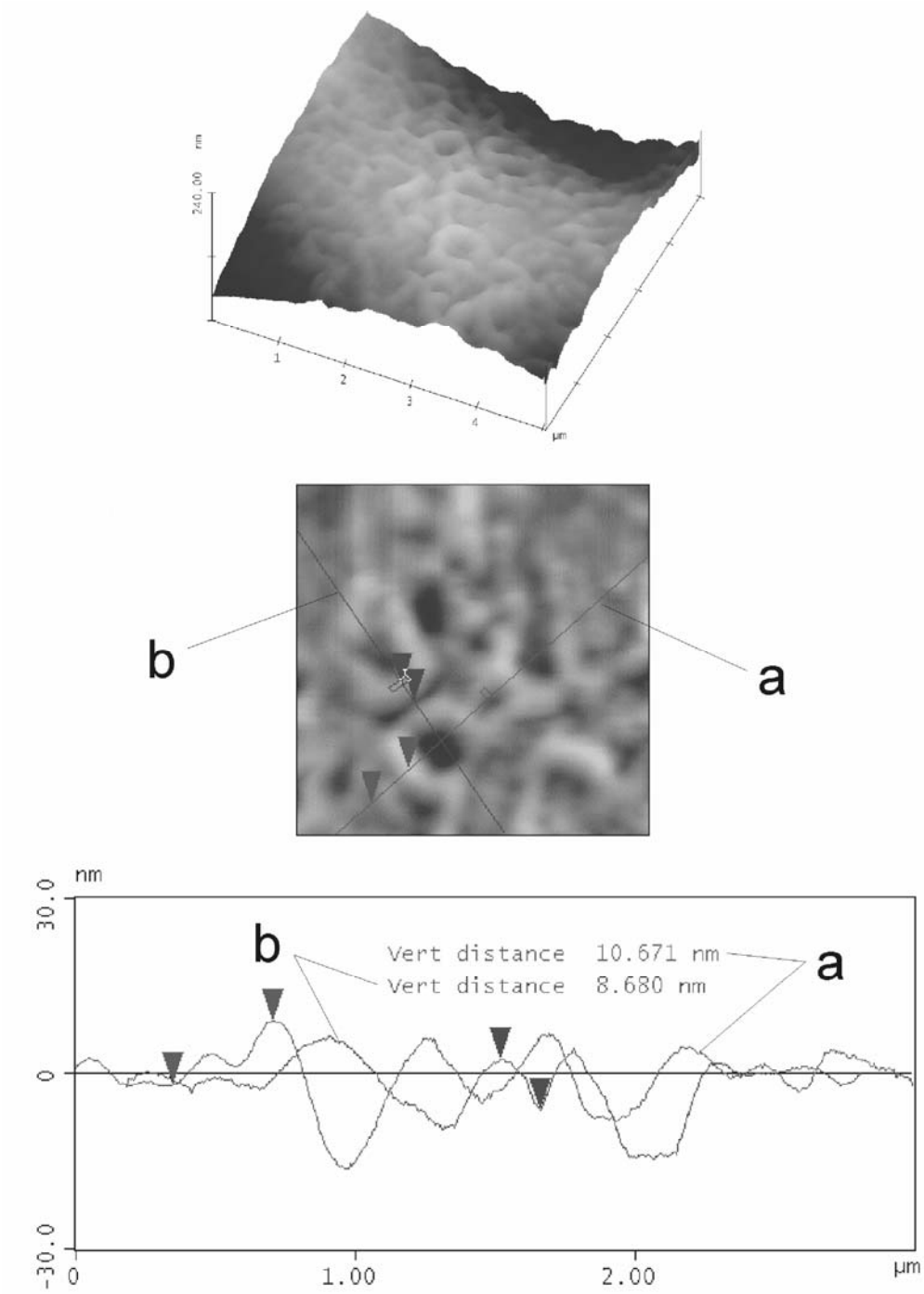

Fig. 5. SFM images of **1** on quartz: an overview, and cross-section analysis (the straight lines represent the directions in the sample taken into consideration in the profile analysis)

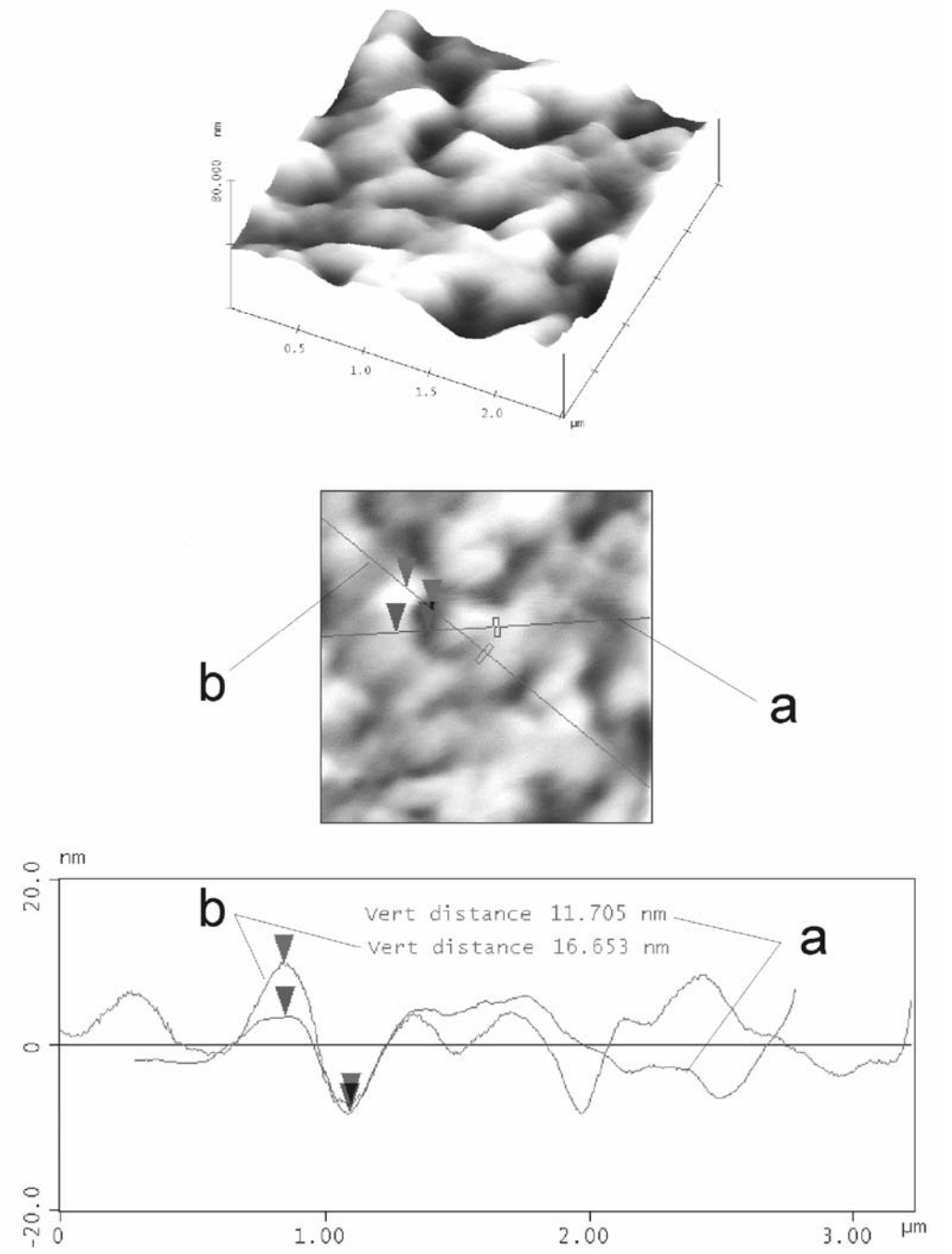

Fig. 6. SFM images of **1** on In_2O_3: an overview, and cross-section analysis (the straight lines represent the directions in the sample taken into consideration in the profile analysis)

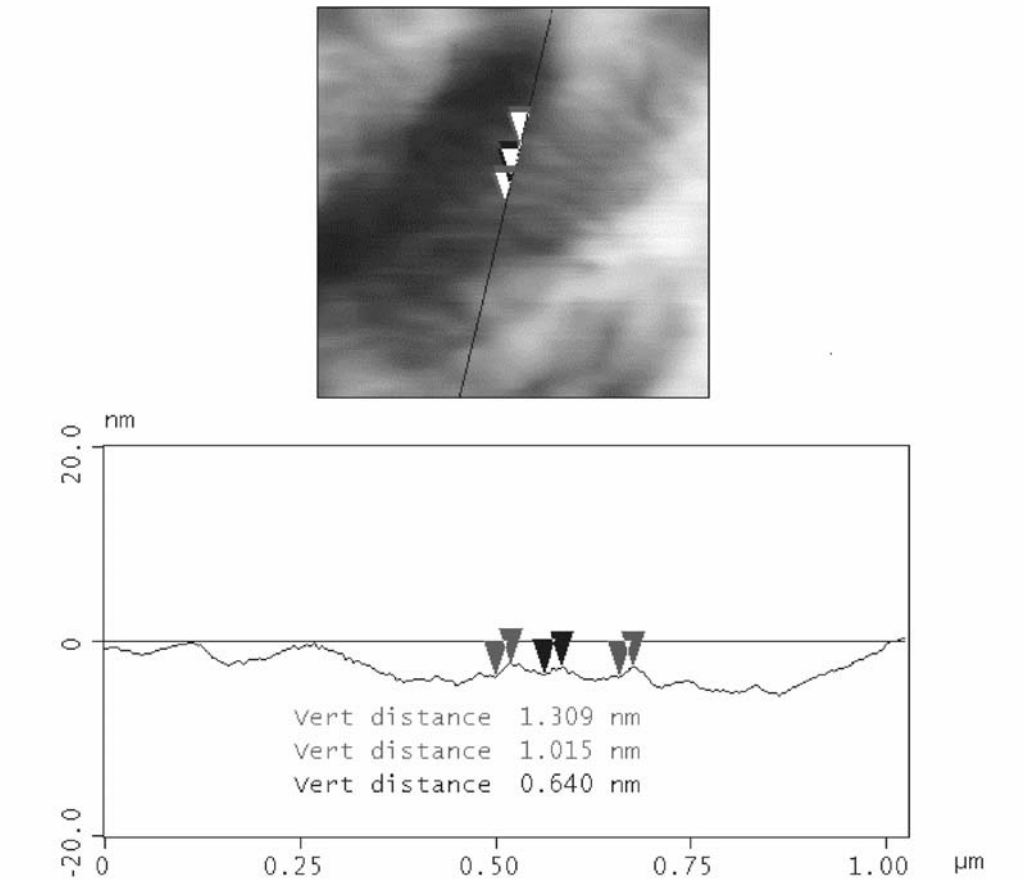

Fig. 7. The cross-section analysis of SFM images of **3** on quartz. The straight lines represent the directions in the sample taken into consideration in the profile analysis

The surface of the dye–polymer system **3** can be seen in Fig. 7, which presents the SFM image of this sample on a quartz plate. The sample is characterized by a longitudinal topography, in which the dye–polymer chains are observed. Basing on the cross-section analysis of surface **3**, we find that the average value of polymer chain height is about 1.1 nm. Figure 8 confirms again the longitudinal structure of sample **3** on the In_2O_3 surface. The section analysis is also shown. A complex profile of the surface topography indicates a multicomponent structure of the dye–polymer with the thickness of about 12 nm with respect to a pit of the In_2O_3 grain. The values of 2.5 nm and 5 nm could describe the layer-by-layer thickness jumps of the polymer on the substrate. These values could be correlated with the van der Waals radius of the PEG chain, being about 3.5 nm [25].

The cross-section results indicate that the final morphologies of the thin films in the dye–polymer systems are affected by the kind of the sample and by the original topography of the substrate.

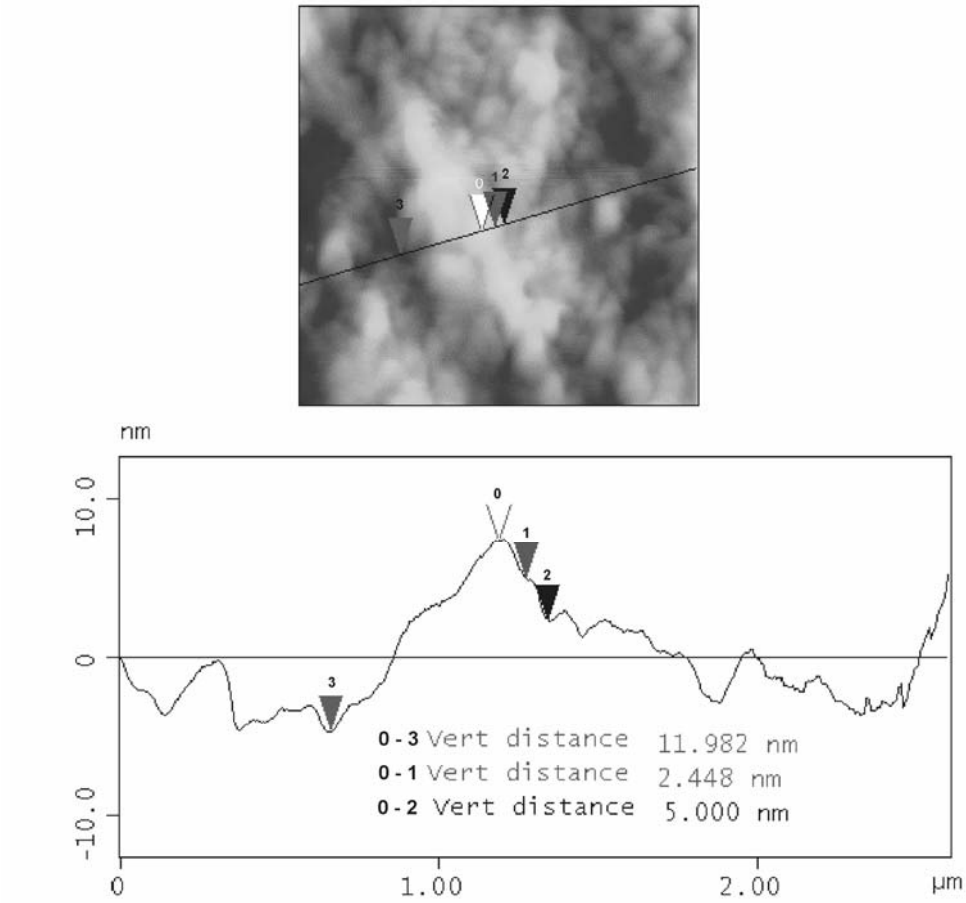

Fig. 8. The cross-section analysis of SFM images of **3** on In_2O_3. The straight lines represent the directions in the sample taken into consideration in the profile analysis

4. Discussion

A general idea of this paper was to show that the optical microscopy and SFM images of polymeric samples are affected by their molecular structure, by polymer length, and by the population of dye molecules covalently linked to the polymeric chain. To find a correlation between the variation of the final images of dye–polymer systems and the granularity of the substrates, one has to consider several effects and factors:

- the relation between the granularity of the substrate and the size of the dye –polymeric systems,
- differences between molecular structures of various dye–polymeric systems; samples **1**, **2**, and **3** differ in their polymer chain structure, polymer chain length, and in their population of dye molecules along the chain,

• differentiation of the orientation of dye–polymer samples with respect to the substrate surface.

Samples **1** and **2** are characterized by a rather homogeneous topography when deposited on a quartz plate or In_2O_3. This effect could be discussed in terms of the dye dimensions and dye orientation with respect to the substrate. The size of these polymeric samples are suitable for quartz and In_2O_3 granulites. Every dye–polymer system exhibits different topography when deposited on solid surfaces: the dye–polymer **1** shows a ring-like structure, whereas the dye–polymer **3** presents a dendritic surface structure with well observed crystallized grains. In the case of the dye–polymer **1**, the ring–like structure lies almost flatly on the quartz and In_2O_3 substrates (the tilt angles are 90 and 130, respectively), owing to the rather low granularity of In_2O_3. On the other hand, although the polymer **3** has a dendritic structure, its chains also lie flatly on the In_2O_3 surface due to low In_2O_3 granularity. Similar results were also observed for much smaller molecular materials (phthalocyanines) [9, 15], and these new results confirm our previous observation.

We have also shown that the substrate with large grains (SnO_2) exhibited a tendency to preserve its own topography. Although the investigated dye–polymer systems differ essentially in their molecular structures and sizes, the image of the SnO_2 surface is rather weakly changed after coating it with the macromolecular materials due to the original large grains. It is evidently seen for the dye–polymer **3**; the original topography is still preserved, and this could be interpreted to be caused by filling the troughs between SnO_2 grains by perpendicularly oriented dyes and dendritic polymers. This polymer is thus not seen on the surface of large grains upon SFM examination. Studying dye–polymers deposited on SnO_2, however, is difficult due to a high roughness of the substrate. Small changes in the SFM image of SnO_2 were also observed after the surface was coated by some porphyrin and phthalocyanine dyes. These changes are discussed in terms of the large grain of SnO_2 and out-of -plane orientation of the dyes with respect to the semiconducting surface [9].

Summarizing, we have shown that the final topography of the dye–polymer layer covering the solid substrate depends predominantly on the molecular structure of the polymer. Also, the granularity of the substrate has a great influence on the final image of the dye–polymer layer. The effect of sample orientation cannot be excluded. In the case of the substrate with large grains (SnO_2), the space between grains is sufficiently large to be filled and covered by the polymer chain. Otherwise, when the substrate has a more homogeneous topography, the polymer is rather flatly deposited on the substrate surface (quartz, In_2O_3).

Acknowledgements

The paper is supported by the Poznan University of Technology, grant BW 62-195/04. The study was also supported by the DAAD/ZIP (grant no. 214/IQN, UAS Wildau, Germany). A. Boguta thanks the Foundation of Polish Science for a Fellowship for Young Scientists. Yu.S. Avlasevich thanks the INTAS for a YSF 2002-362 Fellowship.

References

[1] KNYUKSHTO V.N., AVLASEVICH Y.S., KULINKOVICH O.G., SOLOVYOV K.N., J. Fluorescence, 9 (1999), 371.
[2] GUST D., MOORE T.A., MOORE A.L., IEEE Eng. in Med. Biol., 2 (1994), 58.
[3] ROSENTHAL I., Photochem. Photobiol., 53 (1991), 859.
[4] MOAN J., Photochem. Photobiol., 43 (1986), 681.
[5] SAIKAI Y., SADAOKA Y., MATSUGUCHI M., YOKOUCHI H., TAMAI K., Mat. Chem. Phys., 42 (1995), 73.
[6] GALAEV I.Y., MATTIASSON B., Trends Biotechn., 17 (1999), 335.
[7] PTAK A., DER A., TOTH-BOCONADI R., NASER N.S., FRĄCKOWIAK D., J. Photochem. Photobiol. A, 104 (1997), 133.
[8] WRÓBEL D., BOGUTA A., MAZURKIEWICZ P., Spectrochim. Acta A, 59 (2003), 2841.
[9] BOGUTA A., WRÓBEL D., BARTCZAK A., ION R.M., RIES R., RICHTER A., Surface Sci., 513 (2002), 295.
[10] AVLASEVICH YU.S., KULINKOVICH O.G., KNYUKSHTO V.N., SOLOVYOV K.N., J. Appl. Spectr., 66 (1999), 597.
[11] AVLASEVICH YU.S., CHEVTCHOUK T.A., KULINKOVICH O.G., KNYUKSHTO V.N., SOLOVYOV K.N., J. Porphyrins Phthalocyanines, 4 (2000), 579.
[12] SMITH K.M., *Porphyrins and metalloporphyrins*, Elsevier, Amsterdam, 1975.
[13] SALTER G.J., KELL D.B., ASH L.A., ADAMS J.M., BROWN A.J., JAMES R., Enzyme Microb. Technol., 12 (1990), 419.
[14] GREGORY FOREST M., WANG Q., BECHTEL S.E., J. Rheology, 41 (1997), 821.
[15] CHEN S.B., JIANG L., Phys. Fluids, 11 (1999), 2878.
[16] YONEYAMA M., SUGI M., SAITO M., IKEGAMI K., KURODA S., IZIMA S., Jap. J. Appl. Phys., 25 (1986), 961.
[17] NORDEN B., Appl. Spectr. Rev., 14 (1978), 157.
[18] ŁUKASIEWICZ J., HARA M., NAKAMURA C., MIYAKE J., WRÓBEL D., FRĄCKOWIAK D., J. Photochem. Photobiol. A, 138 (2001), 235.
[19] RICHTER A., RIES R., Mol. Phys. Rep., 21 (1998), 11.
[20] RICHTER A., RIES R., SZULZEWSKY K., PIETZAK B., SMITH R., Surface Sci., 394 (1997), 201.
[21] WEINGRABER H., ABOU-ALY M., *Handbook of Technical Surfaces* (in German), Vieweg&Son, Braunschweig, 1989.
[22] WÓJCIK A., BOGUTA A., AVLASEVICH Y.S., WRÓBEL D., Int. J. Photoenergy, submitted.
[23] WRÓBEL D., ŁUKASIEWICZ J.AND MANIKOWSKI H., Dyes and Pigments, 58 (2003), 7.
[24] BOGUTA A., WRÓBEL D., BARTCZAK A., ŚWIETLIK R., STACHOWIAK Z., ION R.M., Mat. Sci. Eng. B, 113 (2004), 99.
[25] TANAKA S., ATAKA M., ONUMA K., KUBOTA T., Biophys. J., 84 (2003), 3299.

Received 20 October 2004
Revised 4 November 2004